We are IntechOpen,
the world's leading publisher of
Open Access books
Built by scientists, for scientists

6,900
Open access books available

185,000
International authors and editors

200M
Downloads

Our authors are among the

154
Countries delivered to

TOP 1%
most cited scientists

12.2%
Contributors from top 500 universities

Interested in publishing with us?
Contact book.department@intechopen.com

Numbers displayed above are based on latest data collected.
For more information visit www.intechopen.com

CERMETS for Use in Nuclear Thermal Propulsion

Dennis S. Tucker

Abstract

NASA is currently investigating nuclear thermal propulsion as an alternative to chemical propulsion for manned missions to the outer planets. There are a number of materials being considered for use as fuel elements. These materials include tricarbides and CERMETS such as W/UO_2, Mo/UO_2, W/UN and Mo/UN. All of these materials require high temperature processing to achieve the required densities. It has been found that Spark Plasma Sintering is a good choice for sintering these materials to the required densities while maintaining a uniform grain size. In this chapter a brief history of NASA's research into nuclear thermal propulsion will be given, followed by specific research by this author and others to produce CERMET fuels.

Keywords: nuclear thermal propulsion, fuel elements, spark plasma sintering, density, uranium distribution

1. Introduction

Long duration spaceflight can expose astronauts to two major problems. These are extended periods of weightlessness and radiation exposure. Thus, it is necessary to develop alternate means of propulsion to that of chemical propulsion. A reasonable option being studied by NASA is nuclear thermal propulsion (NTP), whereby nuclear fuel elements made from metal/UO_2, metal/UN or tricarbides are being considered. These fuel elements must be capable of operating in excess of 2700 K while being compatible with the propellant, typically hydrogen [1]. From previous studies it was shown that W/UO_2 as a fuel element can be used both in power and propulsion at temperatures as high as 3000 K [2–4]. Two factors need to be considered when producing W/UO_2 fuel elements. The first is the importance of a uniform distribution of UO_2 particles in the tungsten matrix. If one has segregation of UO_2 particles it can lead to hot spots and ultimately failure of the fuel element. The second factor which needs to be considered is the stoichiometry of the UO_2 particles. Maintaining stoichiometry is vital to ensure stability and proper operation of the fuel element. This chapter will detail a brief history of NTP by NASA including fuel element work, followed by more recent research on various fuel systems under consideration.

2. NTP history

As far back as the 1940s, it was recognized that energy from nuclear fission could be used to power spacecraft by heating a working fluid such as hydrogen and provide thrust to the rocket via expansion of the propellant through a rocket nozzle. A simple drawing of an NTP rocket is shown in **Figure 1** below.

Due to the high specific impulse, NTP is considered to be the preferred propulsion method for future manned flights to Mars. Specific impulse (I_{sp}) is a method to measure and compare the efficiency of different propulsion systems. It is determined by the ratio of thrust to the propellant mass flow rate through the engine. The typical NTP engine would have and I_{sp} = 900 s, which is twice that of chemical propulsion systems. During a Mars manned mission the engine would be run for a total of 4 hours. One hour to accelerate from Earth to Mars, followed by a 1 hour deceleration burn. The same burn cycles would occur on a return trip. Thus it is quite critical for the fuel elements to retain their stability during these burns.

The United States was involved in the production and testing of NTP engines during the period of 1955–1972. This was the Rover/NERVA program which tested 20 prototype reactors during this period. These prototypes included fuel test reactors, a safety reactor and prototype engines. **Figure 2** below shows a test of one of the NERVA engines. This engine reached an Isp of ∼850 s during a 2 hour burn. Twenty prototype reactors were ground tested. Fuel forms evolved over the duration of the program [2–9].

The fuel elements used during testing were of varying compositions. These were coated graphite-matrix elements followed by advanced fuel elements consisting of UC-ZrC-C and all carbide elements ((U, Zr)C) [5–8]. Most of the testing was performed using the coated graphite fuel elements. These elements were full length (52″) with a hexagonal cross section (0.75″ flat-to-flat) and 19 axial holes for propellant flow. These elements were arranged to create a cylindrical reactor core. The NERVA/Rover program proved NTP to be a viable technology [9]. Several prototype reactors were produced which survived multiple restarts and power levels over 4000 MW, thrust levels of 250 klbf, maximum propellant outlet temperatures of 2550 K, a maximum net specific impulse of 850 s and over an hour of
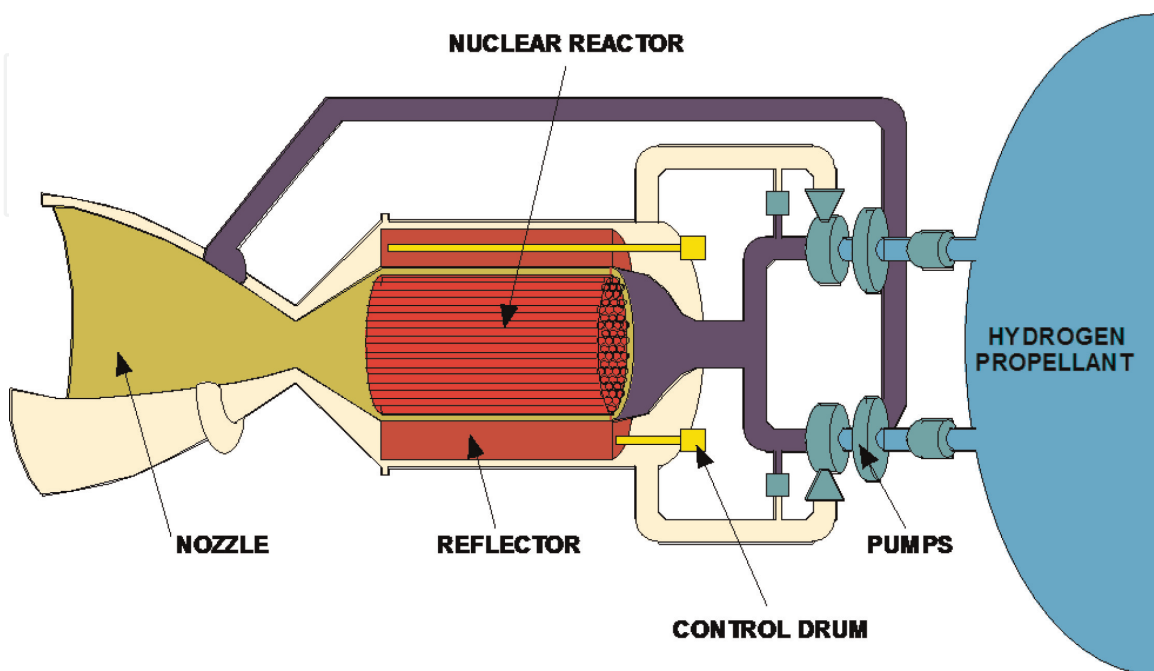

Figure 1.
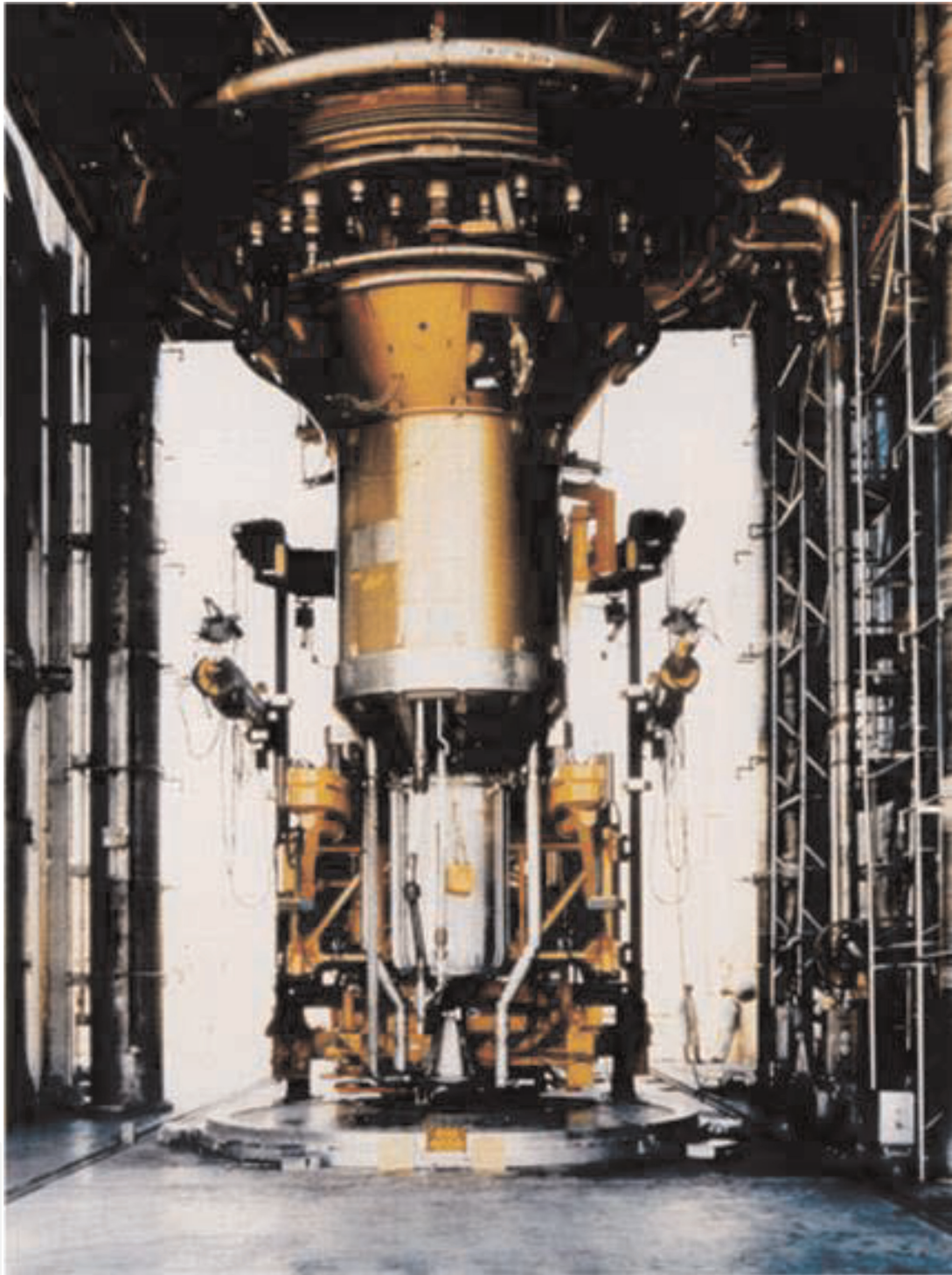*Schematic of NTP rocket.*

Figure 2.
Test of NERVA engine.

continuous operation [9]. The fuel elements had to perform various tasks. The elements contained fissile material (UO_2 or UC_2) and graphite as a moderator. The fuel elements also functioned as structural components.

3. Present-day NTP fuels research

Presently there are a number of fuels under consideration for NTP. These include graphite composites, tricarbides (U-Zr-Nb)C and CERMETS (MUO_2 and MUN). At Marshall Space Flight Center, we are concentrating on CERMETS (W/UO_2, Mo/UO_2, W/UN, Mo/UN) and tricarbides. Consolidation of these

CERMETS and tricarbides has been performed using RF induction furnaces, hot pressing and spark plasma sintering (SPS).

With respect to CERMET processing a number of approaches have been utilized in order to obtain a uniform distribution of the fissile material within the metal matrix. These include traditional powder processing techniques and coating the fissile material with metal using chemical vapor deposition (CVD) [10]. Recently, a fluidized bed reactor to coat UO_2 with tungsten was tested [11]. CVD shows great promise, however, there are technical issues due to the complexity of the experimental CVD apparatus and the CVD process. These issues lead to expense and long reaction times to apply the appropriate thickness coatings. Thus, a technique for obtaining a uniformly coated spherical UO_2 particles was developed [12]. In this technique a small amount of high density polyethylene binder (0.25 w/o) is added to a mixture of tungsten and UO_2 particles. The powders are then mixed thoroughly using a turbula, then heated and mixed on a magnetic stir plate.

Traditional sintering methods can be used to densify W/UO_2. Both hot pressing and hot isostatic pressing have been used. There are drawbacks to these two methods including incomplete sintering and dissociation of UO_2 at high temperatures, pressures and long sintering times. Another issue is a problem of exaggerated grain growth which can occur under these processing conditions.

A sintering method which has been shown to be a reasonable alternative to these traditional method is Spark Plasma Sintering (SPS) [13–15]. SPS leads to higher densities at lower temperatures and processing times while minimizing grain growth. Grain growth is detrimental to densification during the sintering process. In one study, UO_2 was produced by hot pressing, however it was found that a large number of pores were present on the grain faces which led to a smaller grain boundary contact area [16]. In this same study it was observed that grains which had not undergone exaggerated grain growth had pores at the grain corners. It has been observed that pores located on grain faces have greater mobility than those at grain corners and ultimately end up within the grains [17, 18]. Joule heating is utilized in SPS which results in passing a current through the powder during sintering [19]. A pulsed current is utilized in SPS which leads to two different operating temperatures: the average temperature and the maximum temperature. The average temperature is lower than the melting point of the materials. During current discharge, material is transported by a plasma across pores of the matrix. While the pulse is off, the matrix cools rapidly, and this lead to condensation of the material vapor within regions where there is mechanical contact between grains. This mechanism leads to necking between grains. There have been a number of studies have using SPS to consolidate tungsten and a surrogate or tungsten and UO_2. In one study W/CeO_2 was sintered using SPS [19]. In a second study W/UO_2 was densified using SPS [20]. A shortcoming in both of these studies was the segregation of the tungsten and the oxides. In the W/UO_2 study, the materials were mixed in a turbula for 1 hour then hot isostatic pressed [21]. This result was a segregated CERMET due to the differences in powder sizes (W-15 μm, UO_2-200 μm) and density differences where size differences made the largest difference. In **Figure 3** on can plainly see segregation in the sintered CERMET.

Studies [22, 23] were undertaken to eliminate this segregation using an inexpensive, simple technique. Depleted UO_2 particles were obtained from Oak Ridge National Laboratory. These particles had an average size of 200 μm. Tungsten powder with a particle size of 5/15 μm was purchased and used as the matrix material. In order to coat the UO_2 particles with tungsten, a powder processing technique was developed. In this technique, high molecular weight polyethylene powder was milled to approximately 1 μm in diameter. Next a mixture of 50 g of 60 vol% UO_2, 40 vol% W and 0.25 wt% polyethylene powder were thoroughly
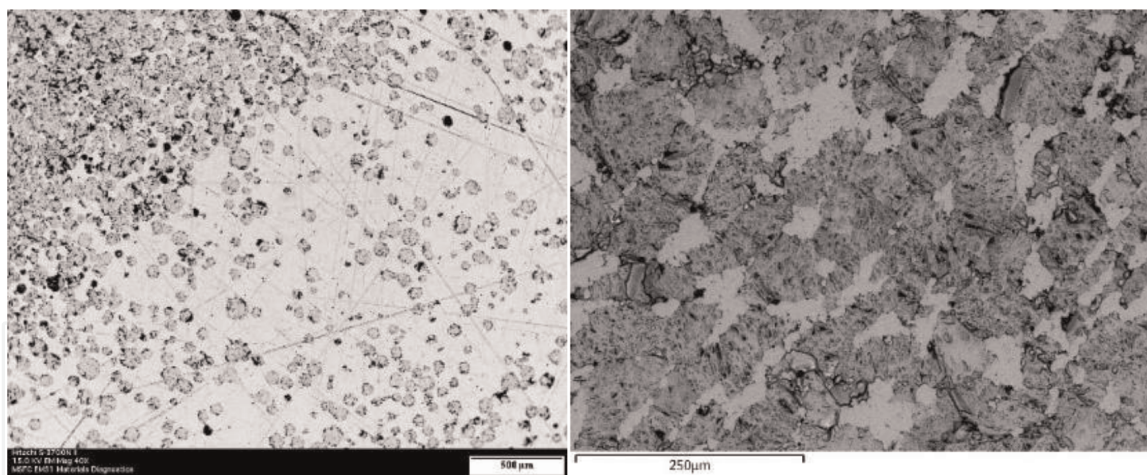
Figure 3.
Scanning electron micrographs of hot isostatic pressed W/UO₂. Dark area on left is UO₂ while on right shows higher magnification image of UO₂.

mixed for 45 minutes in a turbula. This powder was placed in a 400 ml Pyrex beaker and then stirred on a hot plate for 10 minutes above the drop point of the polyethylene (101°C). This process was repeated until 500 g was produced. The powder was shipped to the Center for Space Nuclear Research in Idaho Falls, Idaho for sintering in the SPS. Thirty one grams was placed in a graphene die for sintering. Samples were densified at 1600, 1700, 1750, 1800 and 1850°C. Samples were heated at a rate of 100°C/minute to the sintering temperature. The pressure was increased by 10 Mpa/minute to 50 Mpa. After soaking at the maximum temperature for 20 minutes, the pressure was decreased by 10 Mpa/minute to 5 Mpa and the temperature was decreased by 20°C/minute to room temperature.

Density was obtained using the Archimedes method. Carbon content was analyzed using instrumental gas analysis (EAG, NY). Scanning electron microscopy with energy dispersive x-ray analysis was performed on all samples. Microstructural and chemical analyses were carried out by using transmission electron microscopy (TEM) and atom probe tomography (APT) techniques. TEM and APT specimens were prepared at phase boundaries using lift-out methods with a focused ion beam (FIB). The size of each TEM lamella was 10 × 10 μm. TEM characterization was carried out using a FEI Tecnai G2 F30 STEM FEG equipped with energy dispersive x-ray spectrometry (EDS). The EDS analyses were done in Scanning TEM (STEM) mode with a beam size of 1 nm. APT was carried out using a CAMECA LEAP 4000X HR. APT data reconstruction was done using the CAMECA IVAS software.

Figure 4 shows a scanning electron micrograph of UO₂ particles coated with tungsten powder.

In **Figure 4** one can note that the UO₂ particles are almost completely covered with the tungsten powder. The polyethylene binder is viscous above its drop point (101°C) and coats both the UO₂ particle and tungsten particles which when subsequently mixed together results in the image in **Figure 4**. The mixing temperature was 140°C which led to a binder viscosity of 140 cP. As the mixture was stirred, the nearly spherical UO₂ particles rolled around the bottom of the beaker and were coated with the tungsten particles.

As can be seen in **Table 1** below, the density is relatively high at a sintering temperature of 1600°C and gradually increases up to 1800°C and jumps to 99.46% of theoretical density at 1850°C.

The lower sintering temperature densities align well with what was previously reported for which the density was reported as 97.9% of theoretical for W-Re/UO₂ at 1500°C and 40 Mpa applied pressure using SPS [20]. The higher sintering
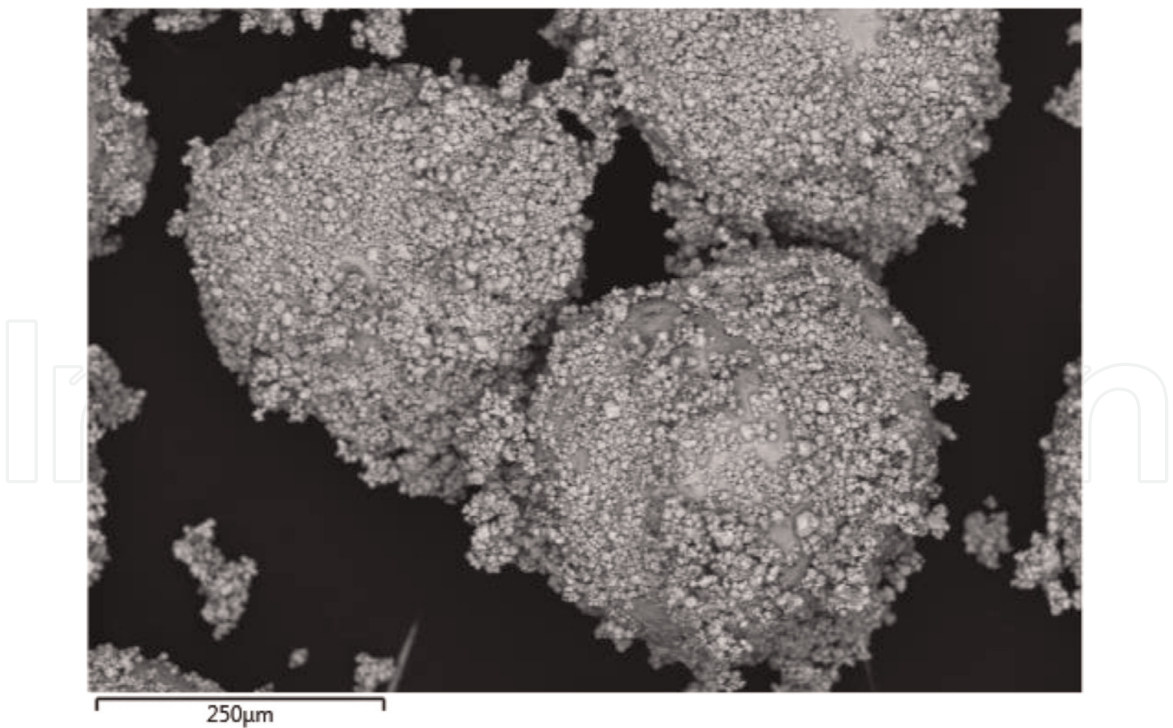
Figure 4.
Scanning electron micrograph showing UO₂ particles coated with tungsten powder.

Sintering Temperature °C	Density, % of Theoretical
1600	97.18
1700	98.19
1750	98.70
1800	98.57
1850	99.46

Table 1.
Sintering temperature versus % theoretical density for SPS W/UO₂.

temperatures and increased applied pressure used in this study can account for an increase in density seen in **Table 1**. It is also thought that decreasing the cooling rate to 20°C/minute could also have contributed to further densification. At lower cooling rated the insulated die will retain heat which will allow more densification.

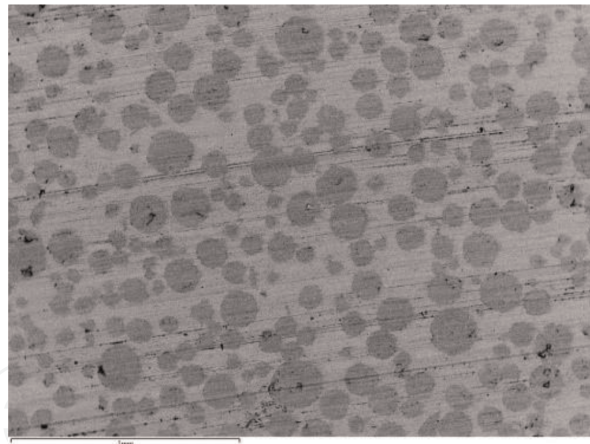**Figure 5** below is a low magnification SEM micrograph of the sample sintered at 1850°C.

Figure 5.
SEM of SPS sintered W/UO₂ at 1850°C.

This figure shows the distribution of UO_2 particles within the tungsten matrix. The UO_2 particles are the darker near spherical particles in the lighter gray tungsten matrix. As can be seen, the distribution of UO_2 particles is nearly uniform with the tungsten matrix. Obtaining a uniform mixture of disparate particle sizes is extremely difficult using traditional powder mixing techniques without the aid of a binder. There four properties which give rise to segregation in powder mixes are: particle size difference, variations in particle density, along with shape and resilience [24]. Particle size difference has been shown to be the most important factor [21]. Segregation of powders causes fluctuations in the size distributions of particles and this leads to variations in bulk density which can affect the desired properties. There are three mechanisms of segregation which can occur during mixing and vibration. Vibration is often used to increase packing density in the powder which in leads to higher sintered densities. Segregation can occur during mixing when fine particles travel further than coarse particles during the mixing operation. If a mass of particles is disturbed so that individual particles move, a rearrangement can take place. This is termed percolation. Over time, gaps between particles occur, which allows particles from above to move down, while a particles from some other location replaces them. When the powder mass contains different size particles, small particles will fall through the large particle interstices leading to segregation. Percolation occurs when the mass of particles is disturbed due to a shear stress within the particle mass. This phenomenon is explained in which a large particle causes an increase in pressure in the region below it which compacts the material and stops the particle from moving downward. Upward movement allows fines to run in under the coarse particle and these in turn lock in position. If the vibration intensity is large enough the larger particles will migrate to the powder surface. The powder process described above which uses polyethylene binder, overcomes this difficulty using a minimum amount of binder which burns out during the SPS process and is drawn away from the sample by the vacuum system. In all the sintering temperatures listed in **Table 1** the vacuum was $\sim 2 \times 10^{-3}$ Torr. The binder acts as an adhesive for the W/UO₂ powders eliminating the disparate particle size effect. It was found that the carbon content for the mixed powders was 0.025 wt%, while the sintered samples were below the detectable limit which is in parts per million.

Figure 6 below shows EDS maps for the sample sintered at 1850°C.

In this figure one can see the SEM in the figure on the left and the x-ray maps on the center and right figure. The UO_2 particles are blue and the tungsten matrix is orange. One can also note some fracturing of the UO_2 particles. This is most likely due to the pressure during sintering but could also be caused during the grinding

and polishing operation. This should be avoided to lessen the probability that uranium can escape and diffuse to the tungsten matrix and to the fuel surface. One can also note some UO_2 particle-particle contact which can lead to hot spots in the fuel during operation. This in turn could lead to disruption of the fuel element.
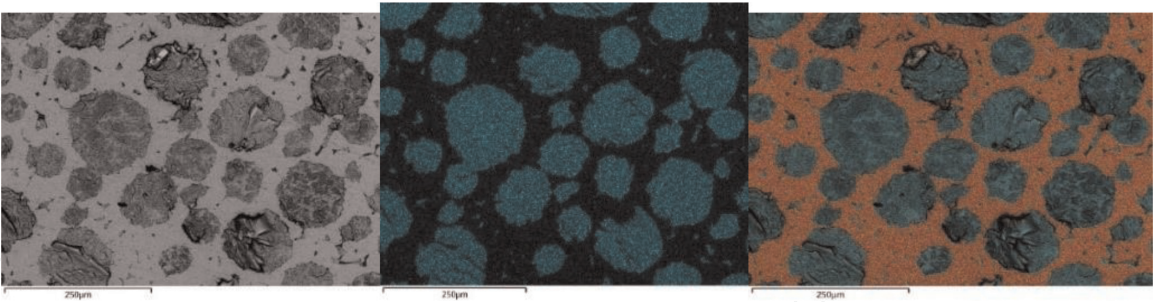

Figure 6.
SEM (left figure), EDS maps (UO_2—blue and W—orange) for sample sintered at 1850°C.
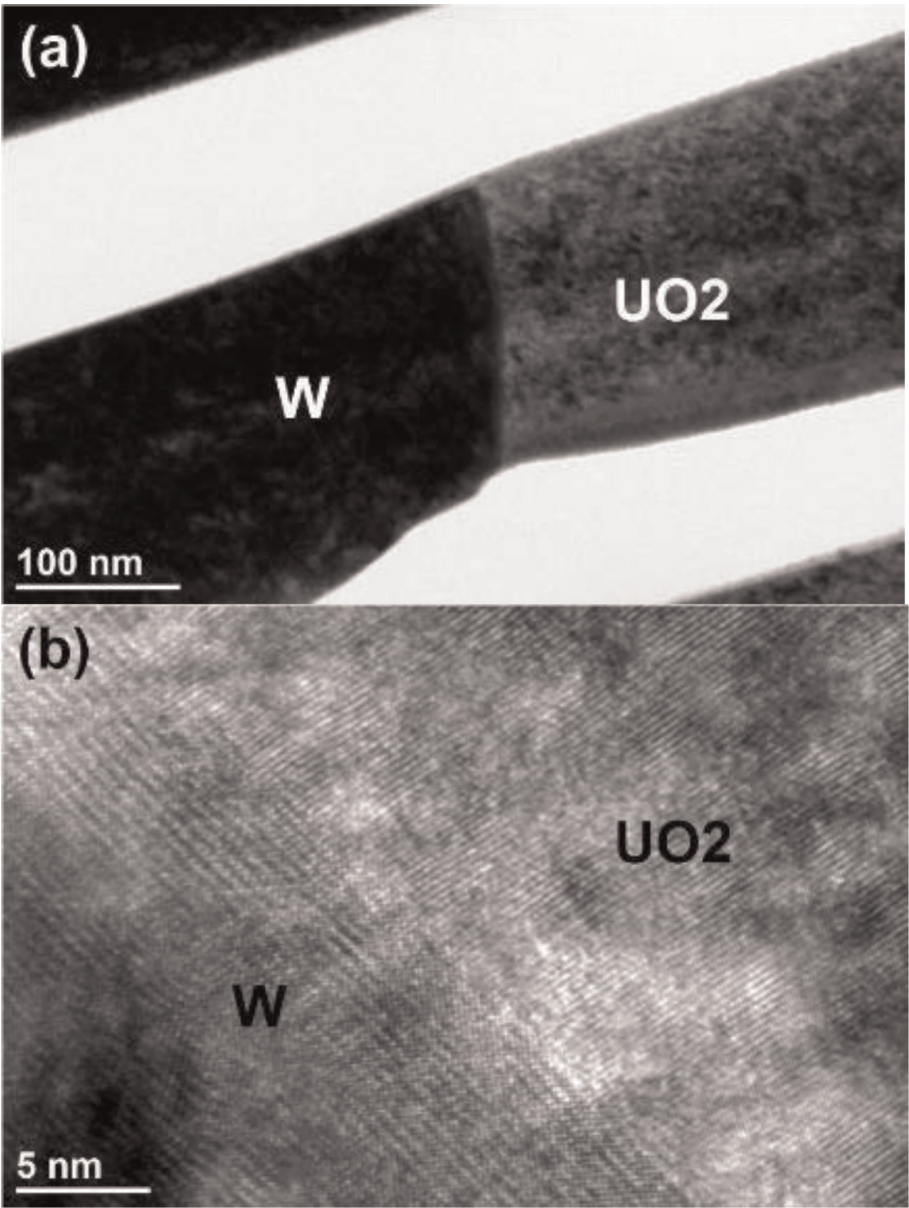

Figure 7.
HRTEM image of boundary of W/UO_2 for sample sintered at 1850°C: (a) is the low resolution boundary and (b) is the high resolution image of this boundary.

Using high resolution transmission electron microscopy (HRTEM) it is possible to image the boundaries between UO_2 particles and the tungsten matrix. **Figure 7** below shows a typical region in the sample sintered at 1850°C.

This type of boundary is typical for all samples except for the one sintered at 1600°C which also showed an anomalous third phase. This is shown in **Figure 8** below.

There was an anomalous phase which was identified as $U_{0.1}WO_3$, space group Pm-3m (221) which is a cubic structure. This was based on its electron diffraction pattern and by considering the atomic ratio of U:W = 1:10 which is consistent with EDS results. Tungsten trioxide, WO_3, has a monoclinic structure with a space group mP32. It is possible that this anomalous phase is WO_3 with uranium contamination, since $U_{0.1}WO_3$ phase has not been previously identified in the literature. Since the space group and crystal structure are different for these two phases, this could be a new phase. High resolution, high intensity x-ray diffraction could be performed on all sintered samples to make a definite determination. It could be that the $U_{0.1}WO_3$ phase forms due to the availability of oxygen vacancies from the UO_2 reduction due to sintering in vacuum. The EDS line scan across the W/UO_2 boundary for the sample sintered at 1850°C is shown in **Figure 9a**.

Figure 9a shows the length of the line scan across the boundary. In **Figure 9b** it can be seen that the uranium has diffused approximately 15 nm into the tungsten matrix. The green line is the uranium curve and one measures where it crosses over the blue curve (tungsten). For all other sintered samples, it was seen that the uranium diffused approximately 10 nm into the tungsten matrix. The atom imaging probe analysis for the sample sintered at 1850°C is shown below in **Figure 10**.

It can be seen from **Figure 10** that the uranium and oxygen were present in the form of UO, UO_2 and UO_3. The nitrogen present is most likely from the nitrogen gas backfill used during SPS at room temperature after cooling. Silicon was observed for all samples except the one processed at 1750°C. Its origin is unknown but most likely is an impurity picked up during grinding and polishing. The carbon present in the sample which is from the polyethylene binder used during powder processing. The above data led to a formula given as $UO_{1.95}$ which is slightly sub-stoichiometric. The samples sintered at 1600, 1650 and 1700°C were also calculated to have this same formula. The only difference was for the sample processed at 1750°C which had the formula UO_2.
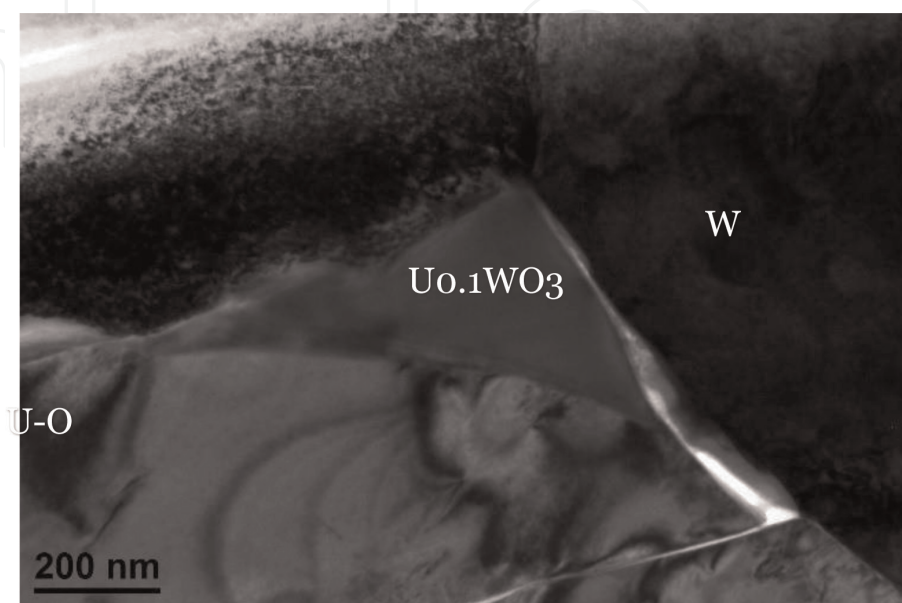

Figure 8.
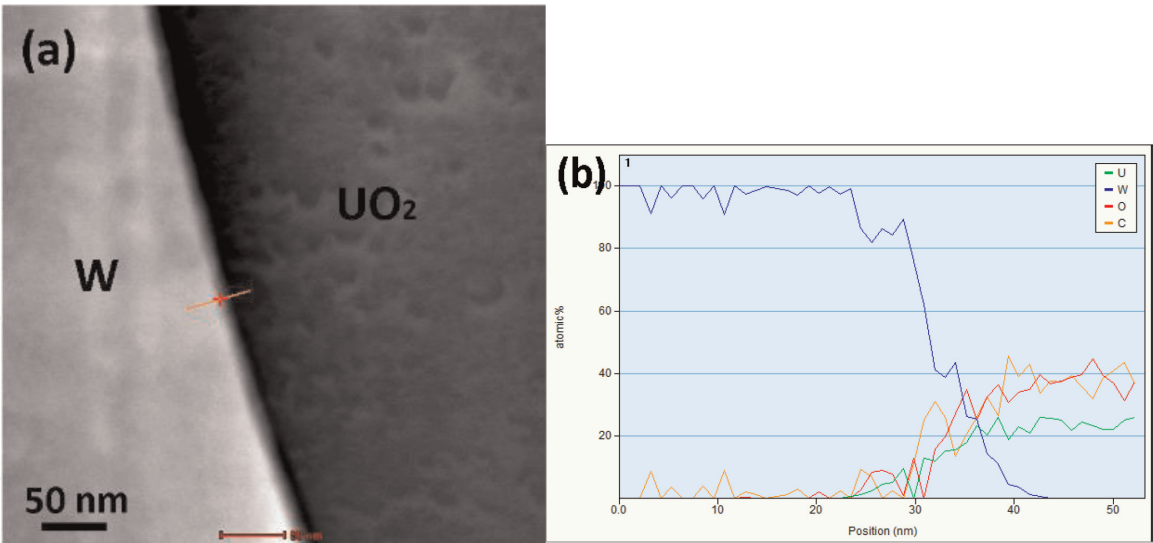*TEM of sample sintered at 1600°C showing phase $U_{0.1}WO_3$.*

Figure 9.
EDS line scan across the W/UO₂ boundary for sample sintered at 1850°C in (a) and the results are in (b).

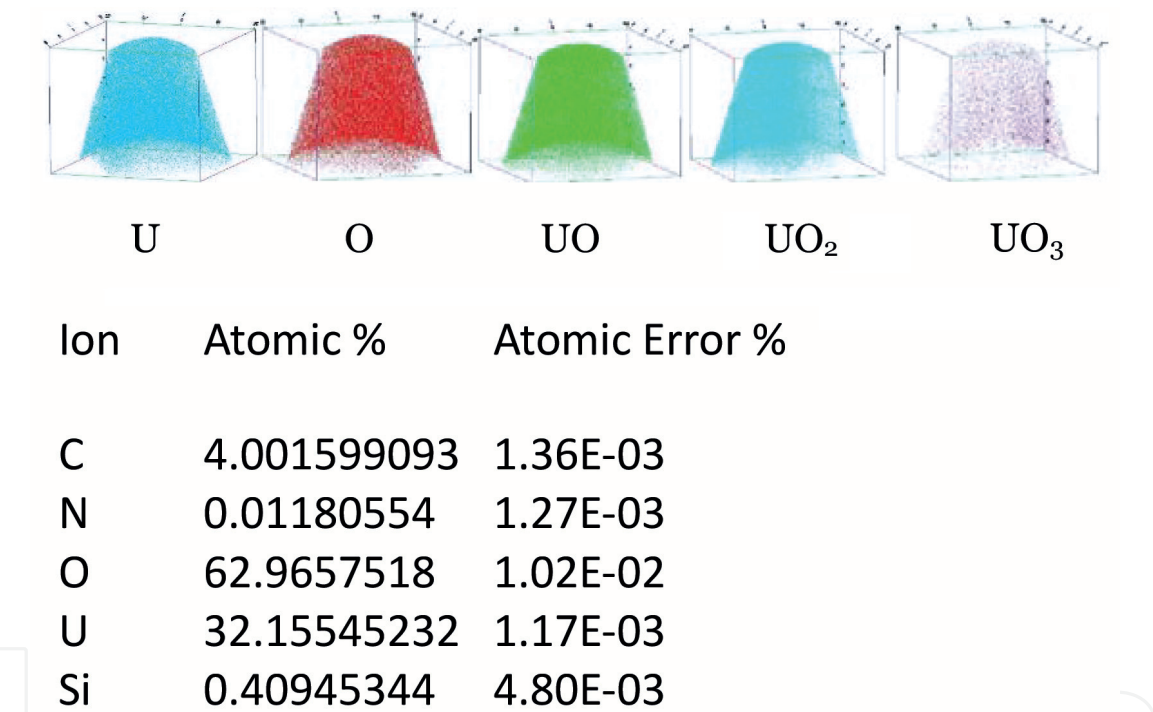| Ion	Atomic %	Atomic Error %
C	4.001599093	1.36E-03
N	0.01180554	1.27E-03
O	62.9657518	1.02E-02
U	32.15545232	1.17E-03
Si	0.40945344	4.80E-03

Figure 10.
3-D element maps from UO₂ particles and atomic percent from sample sintered at 1850°C.

The loss of uranium from the UO_2 particles and uranium migration into the tungsten matrix can be understood in terms of the generation of oxygen vacancies during sintering in a vacuum environment. An reaction for UO_2 if oxygen vacancies are abundant is given by Eq. (1).

$$UO_2 = UO_{2-x} + x/2 O_2 \tag{1}$$

With the loss of oxygen there are two possible defect reactions that can occur. The first reaction is electronic compensation leading to the creation of oxygen vacancies and electrons. This is shown in Eq. (2).

$$O_o = V\ddot{o} + \tfrac{1}{2}O_2 + 2e \tag{2}$$

Ionic substitution can lead to the formation of oxygen vacancies and reduction of the metal oxide on their sites as shown below in Eq. (3).

$$O_o = V\ddot{o} + 1/2O_2 + 2\,M^{'}_M \qquad (3)$$

The result of either of these reactions will be a sub-stoichiometric uranium oxide and free uranium as shown in Eq. (4).

$$2UO_{2-x} \rightarrow (2-x)UO_2 + xU \qquad (4)$$

The free uranium from this reaction is then available to diffuse into the tungsten matrix. This mechanism occurs due to Fick's law of diffusion. The importance of the presence of free uranium in sintered W/UO_2 samples cannot be overstated. These materials will be exposed to hydrogen gas in a thermal cycling environment during engine operation. When thermal cycling takes place in a hydrogen environment, hydrogen will penetrate into the tungsten matrix by both grain boundary and bulk diffusion. The hydrogen can then combine with the free uranium leading to uranium hydride. Uranium hydride can also be formed by reaction with the UO_2 particle. This is shown in Eqs. (5) and (6) below.

$$UO_2 + H_2 \rightarrow UO_{2-x} + xH_2O \qquad (5)$$

$$2UO_{2-x} \rightarrow (2-x)UO_2 + xU \qquad (6)$$
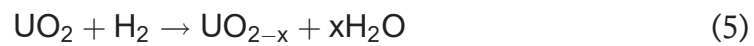
The free uranium has a melting point of $\sim$1130°C and will rapidly diffuse along the tungsten grain boundaries and form UH_3 at $\sim$225°C. The formation of UH_3 leads to large increases in volume and which can result in tungsten grain separation. This grain separation creates avenues for migration of UO_2 to the CERMET surface. This results in the loss of UO_2 and can lead to mechanical failure. The free uranium not only forms UH_3, but can also reoxidize to form UO_2. Both mechanisms result in a large volume expansion and loss of mechanical integrity. There is also a difference between isothermal and cyclic heating. It has been shown that cycling heating results in more fuel loss than isothermal heating in hydrogen [25].

It has been found that oxides such as ThO_2, Ce_2O_3 and Y_2O_3 reduce fuel loss when added to the CERMET powder [25]. The observation was that the oxide additives did not increase the solubility of uranium in UO_2, but stabilized UO_2 against oxygen loss. Two mechanisms were proposed to explain the stabilization against oxygen loss: (1) oxide additives lower the partial molar free energy of oxygen in the UO_2. This precludes the possibility of forming free uranium upon cooling and (2) when metal oxide is added to the CERMET powder, uranium is transformed to a hexavalent state. This hexavalent state precludes the formation of uranium metal. The UO_2 maintains an oxygen-to-metal ration of 2.0–2.1 by forming a defect lattice structure. To maintain electrical neutrality, the uranium ions will be in the hexavalent state. U^{4+} cannot be reduced to the metal in the presence of U^{6+}. Thus, the initial loss of oxygen from the CERMET will be accompanied by oxygen vacancies rather than the formation of free uranium. The use of hyperstoichiometric uranium oxide (UO_{2+x}). UO_2 CERMETS in which the O/U ratio of the starting composition was varied between 1.93 and 2.05 was studied. It was shown in this study that there was minimal effect of varying this ratio. Thus the most likely candidate to stabilize UO_2 during sintering and thermal cycling in hydrogen will be a rare earth oxide addition.

4. Conclusions

In this chapter a brief history of the nuclear thermal propulsion program was given. A present-day research into processing and properties of nuclear fuel

elements was discussed. In particular W/UO$_2$ which was spark plasma sintered was discussed. Uranium migration into the tungsten matrix was observed for all samples. The presence of uranium was explained in terms of oxygen vacancy generation due to processing in vacuum and the migration of the uranium by Fick's law of diffusion. Possible solutions to this problem were also discussed.

Acknowledgements

Conflict of interest

There is no conflict of interest represented by this work.

Author details

Dennis S. Tucker
NASA Marshall Space Flight Center, Alabama, United States

*Address all correspondence to: dr.dennis.tucker@nasa.gov

IntechOpen

References

[1] Burkes DE, Wachs DM, Werner JE, Howe SD. An Overview of Current and Past W-UO$_2$ CERMET Fuel Fabrication Technology. Space Nuclear Conference; 2007

[2] Bhattacharyya SK. An Assessment of Fuels for Nuclear Thermal Propulsion, ANL/TD/TM01-22; 2001

[3] Marlowe MO, Kaznoff AI. Development of Low Thermal Expansion W/UO$_2$ Nuclear Fuel, NASA-CR-72711; 1970

[4] Baker RJ. Basic Behavior and Properties of W/UO$_2$ CERMETS, NASA-CR-54840; 1965

[5] Koenig DR. Experience Gained from the Space Nuclear Rocket Program (ROVER), Rep. No. LA-10062-H; Los Alamos National Laboratory; 1986

[6] Lyon LL. Performance of (U,Zr)C-Graphite (Composite) and (U,Zr)C (Carbide) Fuel Elements in the Nuclear Furnace 1 Test Reactor, Rep. No. LA-5398-MS; Los Alamos National Laboratory; 1973

[7] Wallace TC. Review of Rover fuel element protective coating development at Los Alamos. In: Proceedings of the Eight Symposium on Space Nuclear Power Systems. 1991. pp. 1024-1036

[8] Taub JM. A Review of Fuel Element Development for Nuclear Rocket Engines, Rep. No. LA-5931; Los Alamos National Laboratory; 1975

[9] Qualls L. Graphite Fuel Development for Nuclear Thermal Propulsion; Oak Ridge National Laboratory; 2013

[10] Benensky K. Summary of historical solid Core nuclear thermal propulsion fuels [thesis]. State College Pennsylvania, Penn State University; 2013

[11] Hickman RR, Broadway JW, Mirales OR. Fabrication and testing of CERMET fuel materials for nuclear thermal propulsion. In: AIAA Joint Propulsion Conference; 13 July-1 August 2012; Atlanta, Georgia. 2012

[12] Tucker DS, O'Connor A, Hickman R. A methodology for producing a uniform mixture of UO$_2$ in a tungsten matrix. Journal of Physical Science and Applications. 2015;**5**:255-262. DOI: 10.17265/2159-5348/2015.04.002

[13] O'Brien RC, Ambrosi RM, Bannister NP, Howe SD, Atkinson HV. Spark plasma sintering of simulated radioisotope materials within tungsten CERMETS. Journal of Nuclear Materials. 2009;**393**:108-113. DOI: 10.1016/j.jnucmat.2009.05.012

[14] Wang X, Xie Y, Fuo H, Van der Blest O, Vieugels J. Sintering of WC-Co powder with nanocrystalline WC by spark plasma sintering. Rare Metals. 2006;**25**:246

[15] Atkinson HV, Davies S. Fundamental of hot isostatic pressing: An overview. Metallurgical and Materials Transactions. 2000;**A31**:2981

[16] Xu A, Soloman AA. The effects of grain growth on the intergranular porosity distribution in hot pressed and swelled UO$_2$. In: Proceedings of Ceramic Microstructures '86; July 1986; Plenum, Berkley, CA: University of California. 1986. pp. 28-31. ISBN: 0306426811

[17] Carpay FMA. The effect of pore drag on ceramic microstructures. In: Proceedings of Ceramic Microstructures '76; Westview, Boulder, CO. 1977. p. 171. ISBN: 0891583076

[18] German RM. Sintering Theory and Practice. New York: John Wiley; 1996. ISBN: 0-471-05786-X

[19] O'Brien RC, Ambrosi RM, Bannister NP, Howe SD, Atkinson HV. Safe thermoelectric generators and heat sources for space applications. Journal of Nuclear Materials. 2008;**377**:506

[20] O'Brien RC, Jerred ND. Spark Plasma Sintering of W-UO$_2$ CERMETS; 2013. pp. 433-450

[21] Williams JC. The segregation of particulate materials: A review. Powder Technology. 1976;**15**:245

[22] Tucker DS, Barnes MW, Hone L, Cook S. High density, uniformly distributed W/UO$_2$ for use in nuclear thermal propulsion. Journal of Nuclear Materials. 2017;**486**:246-249. DOI: 10.1016/jnucmat.2017.01.033

[23] Tucker DS, Wu Y, Burns J. Uranium migration in spark plasma sintered W/UO$_2$ CERMETS. Journal of Nuclear Materials. 2018;**500**:141-144. DOI: 10.1016/jnucmat.2017.12.029

[24] Haertling C, Hanrahan RJ. Literature review of thermal and radiation performance parameters for high-temperature uranium dioxide fueled CERMET materials. Journal of Nuclear Materials. 2007;**366**:317-335. DOI: 10.1016/jnucmat.2007.03.024

[25] Saunders NT, Gluyas RE, Watson GK. Feasibility of a Tungsten-Water Mediated Rocket II. NASA Lewis Research Center Report, NASA-TM-X-1421; 1968